Nanophotonic interferometer realizing all-optical exclusive or gate on a silicon chip

Ofer Limon
Zeev Zalevsky
Bar-Ilan University
School of Engineering
Ramat-Gan, 52900
Israel
E-mail: zalevsz@eng.biu.ac.il

Abstract. We present an all optical approach allowing the realization of microscale logic exclusive or (XOR) gate based on special interferometer configuration. The operation device includes two close optical waveguides realized on a silicon chip. A thin metallic layer of a few nanometers that separates the two waveguides causes a relative phase shift of π between them. The structure performs interference of the two input beams while demonstrating XOR logic gate operation at the amplitude of the resulted output. The logic operation is realized after small propagation distance of <1.8 μm. [DOI: 10.1117/1.3156021]

Subject terms: logic devices; integrated optics; interference; optical circuits.

Paper 080911RR received Nov. 21, 2008; revised manuscript received Apr. 30, 2009; accepted for publication May 4, 2009; published online Jun. 24, 2009.

1 Introduction

Photonic data processing and especially photonic devices integrated on silicon chips are becoming a major trend in the world of science and engineering in recent years. This evolution was urged by the microelectronic devices that are reaching their performance envelope and by the fact that the links for the information transmission (i.e., the fibers) use an optical carrier anyhow. Therefore, interfacing those links with photonic modules capable of having faster processing rates and improved immunity to noises is very desirable. All-optical photonic devices and logic gates have been proposed before. The operation principle is based on a nonlinear process, such as two and four waves mixing.[1–3] Those devices can be in various types of substrates.[4] Because microelectronic circuits are realized on silicon chips, the silicon wafers deserve special attention. In silicon, nonlinear operation is realized using nonlinear effects, such as two-photon absorption,[5] plasma dispersion effect,[6] or parametric gain.[7] The realized all-optical devices are usually ring resonators or Mach–Zehnder interferometers.[8] Other available devices include slow light modules,[9] wavelength converters,[10,11] pulse shaping,[12,13] and all-optical switches.[14] Sometimes nonlinear operations as logic gates can also be realized using linear effects as interference if a small number of modules is to be cascaded.[15]

In this paper, we present a novel concept of a miniaturized interferometer used to realize an all optical logic exclusive or (XOR) gate. The logic operation of XOR is very useful for encryption of information in optics communication. The novelty is in the interference configuration. The proposed device contains two wave-guiding cores in silicon separated by a very thin layer of metal having a width of ~16 nm. Because of this layer, the light that is coupled from one core to the next has a relative phase shift of π. This shift is used for the realization of the interference yielding the logic operation. The main advantage of the proposed device is its small interaction length. The all optical logic XOR gate is realized within interaction length as small as 1.7 μm in length.

In Sec. 2, we present the methodology used for designing and simulating the proposed device; the theory and the physical modeling is described in Sec. 3. Numerical simulations are presented in Sec. 4, and the paper is concluded in Sec. 5.

2 Methodology

We performed the design and numerical investigation of the proposed device using R-Soft and COMSOL Multiphysics simulation software. R-Soft relies on the finite difference time domain (FDTD) method. The FDTD approach is based on a direct numerical solution of the time-dependent Maxwell's curl equations. COMSOL Multiphysics is a well-known and proven commercial software that solves the partial wave equation via the finite element method.

Our simulations were preformed for an optical wavelength of $\lambda=1.5$ μm. We solved a 2-D TM mode for the general structure and correlated the results with a full 3-D modeling. Obviously, reducing the optical wavelength results with reduction in the dimensions of the proposed devices.

3 Theory and Modeling

It is a known fact that a structure built out of two identical slab waveguides with a subwavelength separation transfers the light between the two waveguides with a constant phase shift of $\pi/2$.[16] The spatial periodicity of the power transfer between the two waveguides depends on the magnitude of the wavenumber $k=2\pi/\lambda$ with λ being the optical wavelength in the waveguide. The first complete crossing of power from one waveguide to the other occurs when

$$z=L_c=\pi/2k, \tag{1}$$

where L_c is the normalized coupling length.

The waveguiding structure that we propose is made out of two silicon waveguides each 0.2 μm wide and a metal of

0091-3286/2009/$25.00 © 2009 SPIE

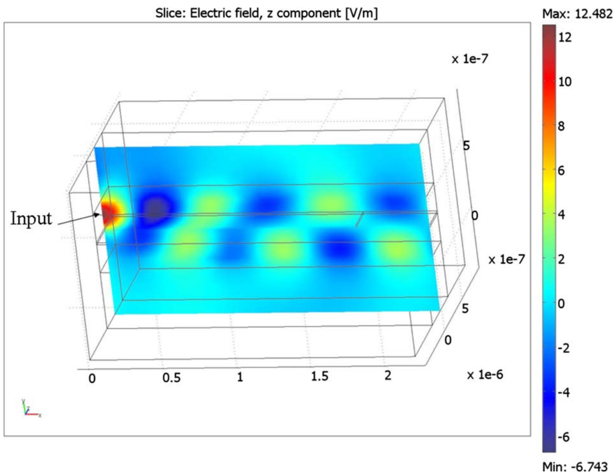

Fig. 1 Phase-locking phenomenon: while tunneling is being preformed, the phase difference between the two channels is starting from $\pi/2$, which corresponds to regular coupled mode structure and at the end of the device the two single modes are propagating simultaneously while the phase difference is locked to π.

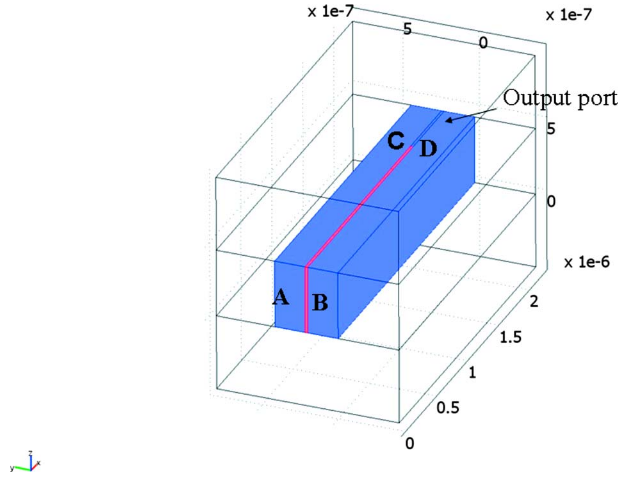

Fig. 2 Scheme of the all-optical logic XOR gate. The blue rectangles are 200×450 nm silicon waveguides, a 16 nm metal is etched in-between, along length of 1.7 μm; it is marked in red. The output signal is obtained at the last 0.5 μm, where a continuous silicon waveguide is established along $\hat{y}$ axis with no metallic perturbation. The structure is surrounded by air gaps on top and sides and SiO_2 at the bottom. Ports A and B are inputs while ports C and D are temporary outputs. The output port is obtained at the top end of the structure.

16 nm wide etched between them. The refractive index of the metal has both real and imaginary parts, where the real part changes the phase of a signal and the imaginary one causes absorption.

According to the coupling mode theory,[16] when we confine light at one input there is a coupling between the two waveguides, such that after normalized coupling length the energy is divided between the two waveguides according to the metal width, while the phase shift between the light guided in the two waveguiding cores is π. For $z>L$, we will see in each waveguide a propagation of a single-mode beam without any energy crossing between them and with a locked relative phase. The energy across the longitudinal Z-axis will remain constant after the normalized coupling length. This effect may be well seen in the simulation of Fig. 1, which was realized using the COMSOL Multiphysics 3-D model. Figure 1 presents the discussed phase lock phenomenon.

For the simulations, we chose a typical optics communications carrier wavelength of $\lambda_0=1.55$ μm. One can see that at $z=\lambda=430$ nm, the contrast between the channels is high because the tunneling of the energy is yet to be completed. The phase shift is $\pi/2$, which is similar to the phase shift obtained in the regular coupled mode structure. At $z=2\lambda$, the energy tunneling is almost accomplished and an equilibrium is about to be established while the relative phase shift is already $3\pi/4$. After a propagation distance of $z=4\lambda$, the tunneling has been accomplished, the energy is equally divided between the two channels, and the relative phase shift is now being set to π. After the phase shift has reached π, no more energy is being lost through the metal and the energy the across Z-axis remains constant.

Note that although the thin metal layer creates the π phase shift effect, it also inserts some energetic attenuation. From the numerical investigation that we have performed, we obtained that there is a loss of 37% of the energy in comparison to an air gap of 16 nm positioned between the two waveguides.

4 Numerical Simulations

The schematic structure of the proposed XOR gate device is depicted in Fig. 2. Two single-mode silicon (with refraction index of $n=3.48$) waveguides with 200×450 nm cross-section are coupled through a 16×450 nm high absorbing material. We modeled the metallic slot by real and imaginary refractive indexes $n=5-6j$ that can, for instance, be realized via cobalt or platinum at 0.8 eV.[17] The clad is taken as 500-nm air gaps on both sides and top of the silicon waveguides. The substrate is a 500 nm SiO_2 (with refraction index of $n=1.48$). A selectively dense meshing is assigned at the slot and slot interface to sample the metallic perturbation according to Nyquist–Shannon sampling theorem. The length of the proposed device is 1.7 μm. The output ports are coupled to a 416×450 nm multimode silicon waveguide with no metallic perturbation. Please note that the energy in the simulation is guided in the $\hat{x}$-axis. According to the operation principle that has been described, the coupling of optical signal to input A generates the propagation distribution as shown in Fig. 1 (i.e., eventually its energy is coupled to the right waveguide with relative phase shift of π). The amplitudes at output ports C or D will be equal. By symmetry considerations, the input signal at port B will lead to the same output at ports C or D as the input at A.

For the case when we input energy at both input ports A and B (inputs with equal amplitudes), the output energy obtained at output ports C or D depends on the relative phase shift between the two inputs: if the phase shift is zero, then both output ports will show zero energy [see Fig. 3(a)]; if the phase shift is π [see Fig. 3(b)], then the energy at both output ports will be equal. The output of our XOR gate device is coupled to the multimode silicon waveguide at the end. High energy is obtained at C or D when inputs A and B differ from each other at their amplitudes and have

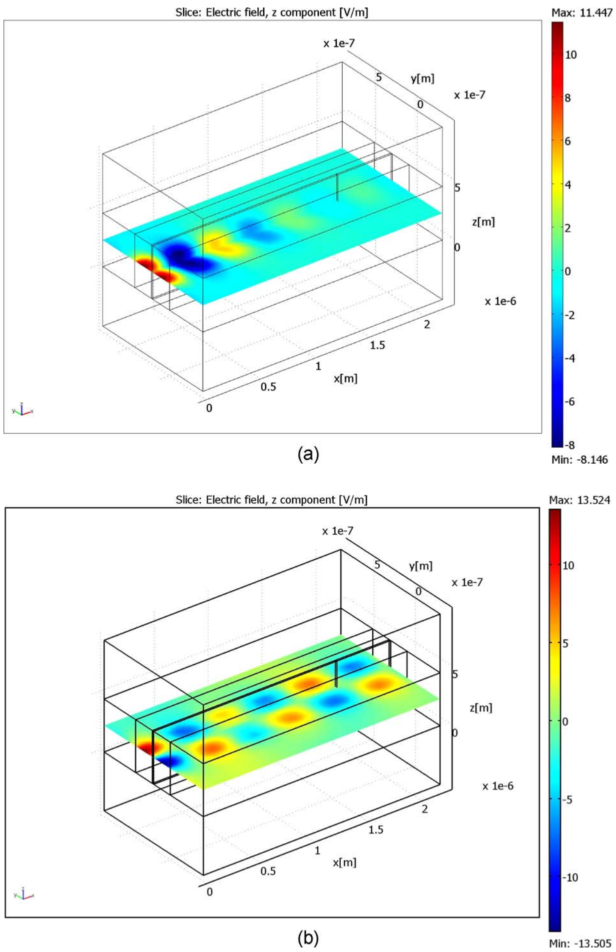

Fig. 3 Numerical characterization. (a) Same energy at ports A and B. Both inputs have equal phase. The energy at the output is zero. (b) The same energy at the inputs while the phase shift is π. Most of the energy is transferred to the output. The losses can be controlled by the width of the metal and the structure of the device.

Table 1 XOR logic state tables. The indicated numbers are the amplitude and the phase in each case. Ports *A* and *B* are the input ports. Ports *C* or *D* may be used as our outputs.

Amplitude input			
Port A	Port B	Port C	Port D
$0\angle 0°$	$0\angle 0°$	$0\angle 0°$	$0\angle 0°$
$0\angle 0°$	$1\angle 0°$	$0.25\angle\theta$	$0.25\angle\theta+\pi$
$1\angle 0°$	$0\angle 0°$	$0.25\angle\theta+\pi$	$0.25\angle\theta$
$1\angle 0°$	$1\angle 0°$	$0\angle 0°$	$0\angle 0°$
Phase input			
Port A	Port B	Output amplitude	
$1\angle 0°$	$1\angle 0°$	0	
$1\angle 0°$	$1\angle\pi$	1	
$1\angle\pi$	$1\angle 0°$	1	
$1\angle\pi$	$1\angle\pi$	0	

the same phase. When both inputs *A* and *B* are equal (e.g. both are 1 or both are 0) the obtained output will have low energy (as summarized in Table 1).

Figure 4 shows how the phase between a *source* and *victim* waveguides depends on the metallic slot conductance. A single port is active (source) and the other port (victim) is idle. As tunneling occurs, the graph reveals how the phase at the end of the all-optical XOR logic gate changes between the source and victim channels. To reach full modulation (i.e., constructive/destructive interference), a phase difference of π should be manifested. Therefore, a proper conductance should be selected according to

$$n = n_r + jn_i, \tag{2}$$

where n is the complex refractive index with n_r and n_i being its real and imaginary (absorption) parts, respectively. Using Eq. (2), one may obtain ε_r, which is the relativistic static permittivity,

$$\varepsilon_r = \varepsilon' + j\varepsilon'', \quad \varepsilon' = n_r^2 - n_i^2, \quad \varepsilon'' = 2n_r n_i. \tag{3}$$

The metal conductivity σ can be defined as follows:

$$\sigma = \omega\varepsilon_0\varepsilon'', \tag{4}$$

where ω is frequency of light and ε_0 is the electric constant.

Basically, the realized device is a miniaturized interferometer while the thin metallic layer is used to produce the desired relative phase shift of π needed for proper interference between the two input ports.

Note that in order to manifest XOR logic, inputs *A* and *B* should have the same phase and the logic operation applies upon its amplitude variations. Because only the output amplitude realizes the XOR logic operation, the output of

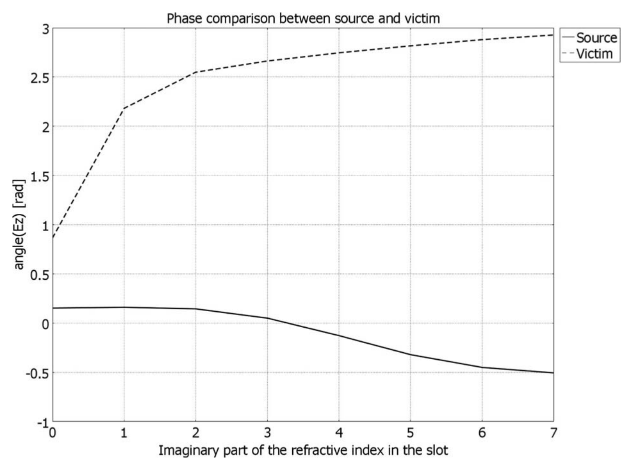

Fig. 4 Phase comparison between "source" and "victim" waveguides for different complex value of the refractive index. The solid line depicts the phase of the source output port at the end of the device, and the dashed line shows the equivalent phase for the victim waveguide. The graph shows the phase modulation dependency on the metallic slot conductance. A full-phase modulation $\Delta\varphi=\pi$ can be achieved for imaginary part of refractive index of 6.

the device should be connected to a detector and, in that way, the output phase information will not have any effect.

Table 1 describes the all-optical XOR gate, for both amplitude input and phase input. This gate can work as fast as the rate at which the input signals are modulated. The device itself adds a delay of 20 fs, caused due to its length and the effective refractive index of the waveguide.

5 Conclusions

A miniaturized special interferometer configuration was used to realize the all-optical logic XOR gate. The operation principle is based on an interesting effect in which a thin conducting nanowire separating two silicon waveguides causes the generation of relative phase shift of π after coupling between the waveguides. The operation rate of the XOR gate is limited by the modulation rate of the input signals with a latency of only 20 fs (the length of the device is $<1.8\ \mu\text{m}$).

The device can be fabricated using conventional tools used in the field of microelectronics. The fact that it is generated on a silicon chip allows its integration with other microelectronic processing circuitry. The small dimensions of the proposed device may provide great benefit to fields such as optics communication and data processing applications facilitating optical integrated circuits.

References

1. C. Luo, J. D. Joannopoulos, and S. Fan, "Nonlinear photonic crystal micro devices for optical integration," *Opt. Lett.* **28**, 637–639 (2003).
2. H. W. Tan, H. M. Van Driel, S. L. Schweizer, R. B. Wehrspohn, and U. Gösele, "Tuning a 2-D silicon photonic crystal using nonlinear optics," presented at Conf. on Laser and Electro-Optics 2004 IFD2, Optical Society of America, Washington DC (2004).
3. H. Fukuda, K. Yamada, T. Shoji, M. Takahashi, T. Tsuchizawa, T. Watanabe, J.-I. Takahashi, and S.-I. Itabashi, "Four-wave mixing in silicon wire waveguides," *Opt. Express* **13**, 4629–4637 (2005).
4. V. Van, T. A. Ibrahim, K. Ritter, P. P. Absil, F. G. Johnson, R. Grover, J. Goldhar, and P.-T. Ho, "All-optical nonlinear switching in GaAs-AlGaAs micro ring resonators," *IEEE Photonics Technol. Lett.* **14**, 74–76 (2002).
5. H. K. Tsang, C. S. Wong, T. K. Liang, I. E. Day, S. W. Roberts, A. Harpin, J. Drake, and M. Asghari, "Optical dispersion, two-photon absorption and self-phase modulation in silicon waveguides at 1.5 μm wavelength," *Appl. Phys. Lett.* **80**, 416–418 (2002).
6. V. R. Almeida, C. A. Barrios, R. R. Panepucci, and M. Lipson, "All optical control of light on silicon chip," *Nature (London)* **431**, 1081–1084 (2004).
7. M. A. Foster, A. C. Turner, J. E. Sharping, B. S. Schmidt, M. Lipson, and A. L. Gaeta, "Broad-band optical parametric gain on a silicon photonic chip," *Nature (London)* **441**, 960–962 (2006).
8. Q. Xu and M. Lipson, "All-optical logic based on silicon micro-ring resonators," *Opt. Express* **15**, 924–929 (2007).
9. Y. Okawachi, M. Foster, J. Sharping, A. Gaeta, Q. Xu, and M. Lipson, "All-optical slow-light on a photonic chip," *Opt. Express* **14**, 2317–2322 (2006).
10. R. Espinola, J. Dadap, R. Osgood, Jr., S. McNab, and Y. Vlasov, "C-band wavelength conversion in silicon photonic wire waveguides," *Opt. Express* **13**, 4341–4349 (2005).
11. H. Rong, Y.-H. Kuo, A. Liu, M. Paniccia, and O. Cohen, "High efficiency wavelength conversion of 10 Gb/s data in silicon waveguides," *Opt. Express* **14**, 1182–1188 (2006).
12. J. Sharping, Y. Okawachi, J. van Howe, C. Xu, Y. Wang, A. Willner, and A. Gaeta, "All-optical, wavelength and bandwidth preserving, pulse delay based on parametric wavelength conversion and dispersion," *Opt. Express* **13**, 7872–7877 (2005).
13. E. Ciaramella and S. Trillo, "All-optical reshaping via four-wave mixing in optical fibers," *IEEE Photonics Technol. Lett.* **12**, 849–851 (2000).
14. Q. Lin, R. Jiang, C. F. Marki, C. J. McKinstrie, R. Jopson, J. Ford, G. P. Agrawal, and S. Radic, "40 GB/s optical switching and wavelength multicasting in a two-pump parametric device," *IEEE Photonics Technol. Lett.* **17**, 2376–2378 (2005).
15. Z. Zalevsky, A. Rudnitsky, and M. Nathan, "Nano photonic and ultra fast all-optical processing modules," *Opt. Express* **13**, 10272–10284 (2005).
16. A. Yariv, "Coupled-Mode theory for guided-wave optics," *IEEE J. Quantum Electron.* **QE-9**, 919–933 (1973).
17. J. H. Weaver and H. P. R. Frederikse, "Optical properties of selected elements," in *CRC Handbook of Chemistry and Physics*, 84th ed., D. R. Lide, Ed., CRC Press, Boca Raton, pp. 12.133–12.155 (2003).

Biographies and photographs of authors not available.